AP2 transcription factor CBX1 with a specific function in symbiotic exchange of nutrients in mycorrhizal *Lotus japonicus*

Li Xue[a], Lompong Klinnawee[a], Yue Zhou[b], Georgios Saridis[a], Vinod Vijayakumar[a,c], Mathias Brands[d], Peter Dörmann[d], Tamara Gigolashvili[a], Franziska Turck[b], and Marcel Bucher[a,1]

[a]Botanical Institute, Cologne Biocenter, Cluster of Excellence on Plant Sciences, University of Cologne, D-50674 Cologne, Germany; [b]Department of Plant Developmental Biology, Max Planck Institute for Plant Breeding Research, D-50829 Cologne, Germany; [c]Department of Plant Pathology, The Ohio State University, Columbus, OH 43210; and [d]Department of Molecular Biotechnology, Institute of Molecular Physiology and Biotechnology of Plants, University of Bonn, 53115 Bonn, Germany

Edited by Jeffery L. Dangl, University of North Carolina, Chapel Hill, NC, and approved August 15, 2018 (received for review July 31, 2018)

The arbuscular mycorrhizal (AM) symbiosis, a widespread mutualistic association between land plants and fungi, depends on reciprocal exchange of phosphorus driven by proton-coupled phosphate uptake into host plants and carbon supplied to AM fungi by host-dependent sugar and lipid biosynthesis. The molecular mechanisms and *cis*-regulatory modules underlying the control of phosphate uptake and de novo fatty acid synthesis in AM symbiosis are poorly understood. Here, we show that the AP2 family transcription factor CTTC MOTIF-BINDING TRANSCRIPTION FACTOR1 (CBX1), a WRINKLED1 (WRI1) homolog, directly binds the evolutionary conserved CTTC motif that is enriched in mycorrhiza-regulated genes and activates *Lotus japonicus* phosphate transporter 4 (*LjPT4*) in vivo and in vitro. Moreover, the mycorrhiza-inducible gene encoding H^+-ATPase (*LjHA1*), implicated in energizing nutrient uptake at the symbiotic interface across the periarbuscular membrane, is coregulated with *LjPT4* by CBX1. Accordingly, *CBX1*-defective mutants show reduced mycorrhizal colonization. Furthermore, genome-wide–binding profiles, DNA-binding studies, and heterologous expression reveal additional binding of CBX1 to AW box, the consensus DNA-binding motif for WRI1, that is enriched in promoters of glycolysis and fatty acid biosynthesis genes. We show that CBX1 activates expression of lipid metabolic genes including glycerol-3-phosphate acyltransferase *RAM2* implicated in acylglycerol biosynthesis. Our finding defines the role of CBX1 as a regulator of host genes involved in phosphate uptake and lipid synthesis through binding to the CTTC/AW molecular module, and supports a model underlying bidirectional exchange of phosphorus and carbon, a fundamental trait in the mutualistic AM symbiosis.

AP2 transcription factor | CTTC *cis*-regulatory element | phosphate transport | mycorrhizal symbiosis | fatty acid biosynthesis

The arbuscular mycorrhizal (AM) symbiosis is an intimate association between fungi of the phylum *Glomeromycota* and the roots of land plants, which have coevolved for over 400 My (1). A characteristic effect of the AM symbiosis is enhanced uptake of phosphorus in the form of inorganic phosphate (Pi) from AM fungi into the host plant in exchange for photosynthetically fixed carbon (2, 3). After penetration into cortical cells, fungal hyphae form dichotomously branched arbuscules enveloped by the plant periarbuscular membrane (PAM), which serves as interface for nutrient sharing between symbionts. Mycorrhiza-inducible Pi transporters reside in the PAM (4–6) and are required for arbuscule function and maintenance. Defective alleles of *Medicago truncatula MtPT4*, rice *OsPT11*, and maize *ZmPT6* strongly impaired mycorrhizal phosphate uptake pathway (MPU) and accelerated arbuscule degeneration (7–9). Mycorrhiza-inducible Pi transporters belong to the subfamilies I, II, and III of the plant Pi transporter 1 (Pht1) family, which is roughly clustered into four subfamilies (10–12). Subfamily I contains Pi transporters expressed exclusively in mycorrhizal roots; several members of subfamily II and III are mycorrhiza-inducible; subfamily IV consists of Pi transporters from monocots that are not mycorrhiza inducible. Serial deletion analysis of promoter elements demonstrated the regulatory role of the CTTC CRE (CTTCTTGTTC, alternatively named "MYCS," TTTCTTGTTCT) in mycorrhiza-inducible Pi transporter genes (13–16).

The driving force for cellular Pi influx is the proton gradient generated by the H^+-ATPase, which activates H^+/Pi symport across Pht1 transporters in the plasma membrane (17). In *M. truncatula* and rice, mycorrhiza-inducible H^+-ATPase (HA1) is essential for MPU and arbuscule development (18, 19). Moreover, the regulatory role of CTTC CRE in the promoter of a mycorrhiza-inducible H^+-ATPase *SlHA8* gene was demonstrated in tomato (20). Although CTTC CRE is widely present in mycorrhiza-responsive genes, transcription factors targeting CTTC CRE remain elusive.

AP2 family transcription factors belong to the AP2/ERF superfamily and are classified into WRINKLED1-like, APETALA-like, and AINTEGUMENTA-like subfamilies (21, 22). In *Arabidopsis thaliana*, WRINKLED1 (WRI1) regulates genes encoding

Significance

Arbuscular mycorrhizal (AM) fungi promote phosphorus uptake into host plants in exchange for organic carbon. Physiological tracer experiments showed that up to 100% of acquired phosphate can be delivered to plants via the mycorrhizal phosphate uptake pathway (MPU). Previous studies revealed that the CTTC *cis*-regulatory element (CRE) is required for promoter activation of mycorrhiza-specific phosphate transporter and H^+-ATPase genes. However, the precise transcriptional mechanism directly controlling MPU is unknown. Here, we show that CBX1 binds CTTC and AW-box CREs and coregulates mycorrhizal phosphate transporter and H^+-ATPase genes. Interestingly, genes involved in lipid biosynthesis are also regulated by CBX1 through binding to AW box, including *RAM2*. Our work suggests a common regulatory mechanism underlying complex trait control of symbiotic exchange of nutrients.

Author contributions: L.X. and M. Bucher designed research; L.X., L.K., Y.Z., V.V., and M. Brands performed research; T.G. contributed new reagents/analytic tools; L.X., L.K., G.S., M. Brands, P.D., F.T., and M. Bucher analyzed data; and L.X. and M. Bucher wrote the paper.

The authors declare no conflict of interest.

This article is a PNAS Direct Submission.

[1]To whom correspondence should be addressed. Email: m.bucher@uni-koeln.de.

This article contains supporting information online at www.pnas.org/lookup/suppl/doi:10.1073/pnas.1812275115/-/DCSupplemental.

enzymes of late glycolysis and fatty acid biosynthesis through binding to the AW box [CnTnG(n)$_7$CG] during seed maturation, while WRI1, WRI3, and WRI4 are required for cutin biosynthesis in floral tissues (22–25). In AM symbiosis, plants provide carbohydrates and fatty acids to mycorrhizal fungi as a carbon source to maintain the mutualism (26–31). Mycorrhizal host-specific *WRI* genes in *M. truncatula* were designated as *MtWRI5a/b/c*. Like *A. thaliana WRI1*, overexpression of *MtWRI5a/b/c* leads to accumulation of triacylglycerol (TAG) in tobacco leaves (29). Consistently, artificial microRNA silencing of *MtWRI5b* led to a lower level of mycorrhizal colonization (32). Here, we identify mycorrhiza-inducible WRI1-like AP2 transcription factor CBX1, which simultaneously regulates central components of MPU and mycorrhizal lipid biosynthesis through direct binding to the CTTC and AW-box motifs in target gene promoters. We propose that CBX1 is likely to play a central role in the evolution and maintenance of AM symbiosis.

Results

***CBX1* Encodes an AP2 Domain-Containing Transcription Factor that Binds to the CTTC *cis*-Acting Regulatory Element.** To examine the function of the CTTC motif in the *LjPT4* promoter, chimeric constructs of the *LjPT4* promoter with the β-glucuronidase reporter gene (*pLjPT4:GUS*) containing the CTTC motif or its mutated form (mCTTC) were stably transformed into *Lotus japonicus* roots (Fig. 1*A*). The *LjPT4* promoter and a quadruple tandem repeat of CTTCTTGTTC fused to a minimal 35S cauliflower mosaic virus promoter (4*CTTC) directed GUS activity specifically in arbuscule-containing roots, corroborating previous results (14, 33), while the presence of mCTTC led to a significant reduction of *LjPT4* promoter activity (Fig. 1*A* and *SI Appendix*, Fig. S1 *A* and *B*). Occasionally, residual *pLjPT4-mCTTC:GUS* expression was detectable and confined to arbuscule-containing cells (*SI Appendix*, Fig. S1*C*), suggesting the action of alternative *cis* elements in transcriptional activation of *LjPT4* expression. Thus, we demonstrated that the CTTC motif was required but not sufficient for full *LjPT4* promoter activity in mycorrhizal root sectors (Fig. 1*A* and *SI Appendix*, Fig. S1*C*).

To identify transcription factors that directly bind to the *LjPT4* promoter, candidate genes that were responsive to AM fungi *Rhizophagus irregularis* and *Gigaspora margarita* (34, 35) were selected for protein–DNA-binding studies using an electrophoretic mobility shift assay (EMSA). We found that the protein encoded by gene Lj6g3v1048880.1 mediated a distinct shift of promoter DNA and CTTC motif, respectively (*SI Appendix*, Fig. S2 *A* and *B*). The binding was outcompeted by unlabeled CTTC but not mCTTC (Fig. 1*B*). The studied protein is hereinafter referred to as CTTC-BINDING TRANSCRIPTION FACTOR1 (CBX1). CBX1 is an AP2 family transcription factor that belongs to 15 members of the *L. japonicus* AP2 family with typical double AP2 domains (21). Five AP2 transcription factors were up-regulated by AM fungi, including *CBX1*, *WRI5a* (Lj2g3v1338890.1 and Lj2g3v1338880.1), *WRI5b* (Lj1g3v2952280.1 and Lj1g3v2952290.1), *WRI5c* (Lj2g3v1034640.1), and *WRI3* (Lj0g3v0151469.1), which all clustered with the WRI1-like subfamily (*SI Appendix*, Fig. S3) (34, 36). *WRI5a*, *WRI5b,* and *WRI5c*

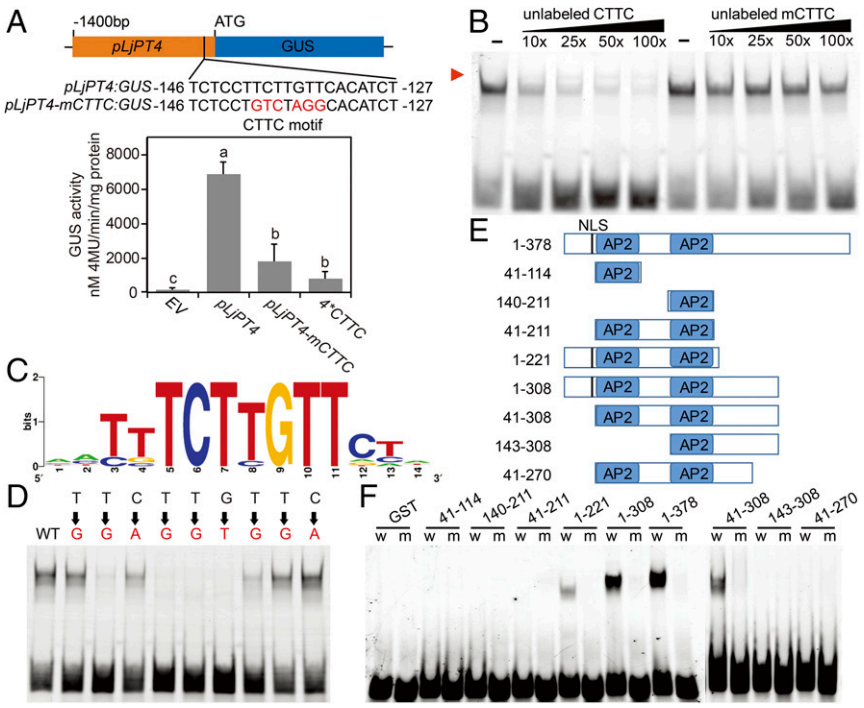

Fig. 1. Sequence-specific DNA-binding properties of CBX1. (*A*) CTTC is required for *LjPT4* gene regulation in mycorrhizal roots. The schematic diagram shows *pLjPT4:GUS* and *pLjPT4-mCTTC:GUS* with mutations (*Upper*). *Lower* shows GUS activity in transgenic hairy roots harboring different reporters in the presence of *R. irregularis*. EV, pRedRoot-GUS vector; 4*CTTC, a quadruple tandem repeat of CTTCTTGTTC fused to minimal 35S cauliflower mosaic virus promoter; 4-MU, 4-methylumbelliferone. Mean ± SD (n = 3). Kruskal–Wallis test followed by Fisher's least significant difference test was used [Kruskal–Wallis χ^2 = 9.7, degree free (df) = 3, $P < 0.05$]. Three independent experiments were performed with similar results. (*B*) EMSA of CBX1 binding to CTTC motif. Unlabeled CTTC CRE or mCTTC CRE were used as competitor. Increasing amounts of competitor DNA is indicated on top. Red arrow indicates the protein–DNA complex. (*C*) The sequence logo of CTTC CRE was created from 21 putative CTTC motifs in promoters of 19 mycorrhiza-inducible Pi transporter genes shown in *SI Appendix*, Table S2 using WebLogo (weblogo.berkeley.edu/logo.cgi). Stack height represents the degree of conservation and the letter size represents relative frequency. (*D*) CBX1 DNA-binding preference for the CTTC motif in EMSA. Nine Cy5-labeled oligonucleotides carrying single base-pair substitutions were synthesized. WT, wild type CTTC motif; red letters, base changes within CTTC; black letters, wild-type bases. (*E*) Schematic diagram of truncated CBX1 proteins. AP2, APETALA2 domain; NLS, nuclear localization signal. Protein regions are labeled at left. (*F*) Relative binding affinities of truncated CBX1on CTTC motif (w) or mutated CTTC (m) in EMSA.

were induced by overexpression of CBX1 in *L. japonicus* transgenic hairy roots, and their encoding proteins could weakly bind CTTC-containing DNA in vitro (*SI Appendix*, Fig. S2 *A–C*).

To map the CBX1–CTTC motif interaction at single-nucleotide resolution, single base-pair substitutions within the CTTC motif (CTTCTTGTTC) were designed for EMSA (Fig. 1*C* and *SI Appendix*, Table S1). The first C in the CTTC motif was not mutated in the synthetic oligonucleotides, as it is not conserved in MYCS (*SI Appendix*, Table S2). EMSA indicated strongly reduced CBX1-binding affinity to CTTC oligomers with base changes at positions T^3, T^5, T^6, or G^7, whereas changes at C^4 or T^8 only moderately affected DNA binding (Fig. 1*D*). Thus, our data indicated that TCTTGT is the core motif fulfilling the minimum sequence requirements for high-affinity DNA binding by CBX1. To determine the protein region(s) in CBX1 responsible for DNA binding, various forms of truncated CBX1 were generated for DNA-binding studies (Fig. 1*E*). Two AP2 domains failed to bind the CTTC element. Comparing the binding ability of CBX $^{1–308}$ and CBX $^{41–308}$ revealed a limited effect of the N terminus encompassing 40 amino acids. The presence of the domain spanning amino acids 212–308 in combination with the AP2 domains enabled DNA binding (Fig. 1*F*). In the C-terminal portion of CBX1, an important role in CTTC binding can be attributed to the region spanning amino acids 271–308.

CBX1 Is Required for Proper Mycorrhizal Root Colonization. To investigate the function of CBX1, two mutants *cbx1-2* and *cbx1-3* carrying LORE1a insertions in the last exon or in the 5′ UTR (*SI Appendix*, Fig. S4 *A* and *B*) were examined for mycorrhizal phenotypes grown at low Pi condition (100 μM) in the presence or absence of *R. irregularis* (37) (Fig. 2*A*). Strongly reduced colonization [Total (%)] was observed in both mutant lines relative to wild type at 6 wk after inoculation (Fig. 2*A*). Furthermore, the proportion of root sectors containing fungal arbuscules {[A + V + H (%)] and [A + H (%)]} was significantly lower in the mutant lines than in wild type (Fig. 2*A*). Accordingly, the transcript levels of AM marker genes *LjHA1*, *LjPT4*, and *RAM2* were significantly reduced in both mutants relative to wild type (Fig. 2*B*). Despite strongly reduced transcript levels of *CBX1*, marker gene expression was still inducible in mutants (Fig. 2*B*), suggesting the existence of functionally redundant regulators. Phosphate application suppresses mycorrhization and mycorrhiza-induced transcription factors (34, 38, 39). The reduced marker gene expression in *cbx1-2* mutant was more pronounced under shift Pi (500 μM) (*SI Appendix*, Fig. S4 *C* and *D*). In addition, overexpression of *CBX1* resulted in an increased level of mycorrhization and *LjPT4* expression (*SI Appendix*, Fig. S4*E*). In sum, the results suggested that CBX1 is involved in arbuscule formation and expression of host genes in PAM functioning.

CBX1 Transactivates *LjPT4* in a CTTC CRE-Dependent Manner. To verify the transcriptional activity of CBX1, we studied its subcellular localization and *CBX1* promoter activity. CBX1-YFP and GFP-CBX1 fusion proteins exclusively localized to the nucleus in transgenic hairy roots of *L. japonicus* and *Arabidopsis* cultured cells (*SI Appendix*, Fig. S5 *A* and *C*). Histochemical analysis of 1.9-kb *CBX1* promoter-driven GUS in transgenic hairy roots indicated cell-autonomous expression of *CBX1* exclusively in root sectors colonized by AM fungus *R. irregularis* (Fig. 2 *C–F*). Moreover, *CBX1* and *LjPT4* gene expression patterns correlated in different plant organ types of distinct mycorrhizal status (*SI Appendix*, Fig. S5*B*). Next, a GFP-tagged CBX1 fusion protein was coexpressed with *pLjPT4:GUS* or *pLjPT4-mCTTC:GUS* reporters, or with the *4*CTTC:GUS* or the *4*mCTTC:GUS* construct, respectively, in suspension-cultured root cells of the mycorrhizal nonhost *A. thaliana* (Fig. 3*A*). Enhanced accumulation of the indigo dye (product of GUS activity) in the cells indicated activation of the *LjPT4* promoter by CBX1, while the *LjPT4* promoter containing mCTTC was not activated (Fig. 3*B*). The GFP-CBX1 fusion transactivated the *4*CTTC:GUS* chimeric gene but not the mutated version (*4*mCTTC:GUS*), while GFP alone had no effect on the reporter system.

To show that promoter activation is specific for CBX1, the three AP2 transcription factors WRI5a, WRI5c, and WRI3 fused to GFP were also coexpressed with GUS reporter constructs in the suspension-cultured cells. Except for CBX1, all three AP2 proteins failed to activate the expression of *pLjPT4:GUS* or *4*CTTC:GUS* (Fig. 3*B*). We also found that the two carboxyl-terminal truncations CBX1$^{1–221}$ and CBX1$^{1–308}$, which retained the ability to bind the CTTC motif in vitro (Fig. 1*F*) and localized to the nucleus

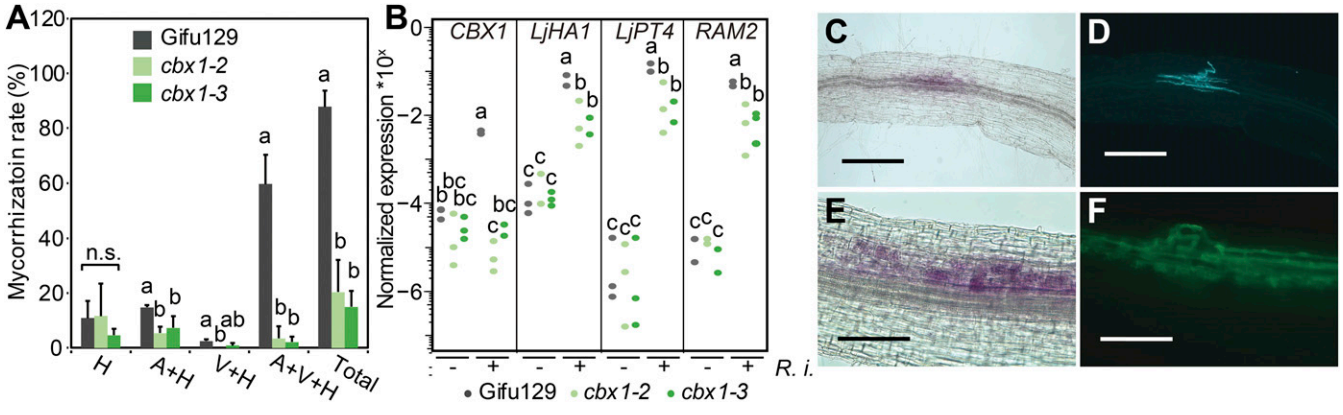

Fig. 2. CBX1 is required for mycorrhizal colonization. (*A*) Mycorrhization rate in Gifu-129, *cbx1-2*, and *cbx1-3* mutant lines grown under low Pi (100 μM) in the presence of *R. irregularis*. A, arbuscules; H, hyphae; V, vesicles; A + H (%), percentage of root sectors with arbuscules and hyphae; A + V + H (%), percentage of root sectors with arbuscules, vesicles, and hyphae; H (%), percentage of root sectors with only hyphae; V + H (%), percentage of root sectors with vesicles and hyphae. Mean ± SD ($n = 3$) is shown. One-way ANOVA followed by Tukey's honestly significant difference (HSD) test was used [F (A + H)$_{2.6} = 9.261$; F (V + H)$_{2.6} = 9.874$; F (A + V + H)$_{2.6} = 70.54$; F (Total)$_{2.6} = 73.2$; $P < 0.05$]. Different letters indicate different statistical groups. n.s., not significant. (*B*) Mycorrhizal gene expression in *cbx1* allelic mutants in the absence (–) or presence (+) of *R. irregularis* ($n = 3$). One-way ANOVA followed by Tukey's HSD test [F (*CBX1*)$_{5.12} = 30.73$; F (*LjHA1*)$_{5.12} = 37.54$; $P < 0.05$] and the nonparametric equivalent Kruskal–Wallis test [χ^2 (*RAM2*) = 15.082; χ^2 (*LjPT4*) = 14.342; df = 5, $P < 0.05$] were used to determine the significance. This experiment was independently repeated three times with similar results. (*C* and *E*) *pCBX1:GUS* activation in *L. japonicus* roots in the presence of *R. irregularis*. (*D* and *F*) WGA488 staining of AM fungal structures in the same sectors. (Scale bars: *C* and D, 500 μm; *E* and *F*, 200 μm.)

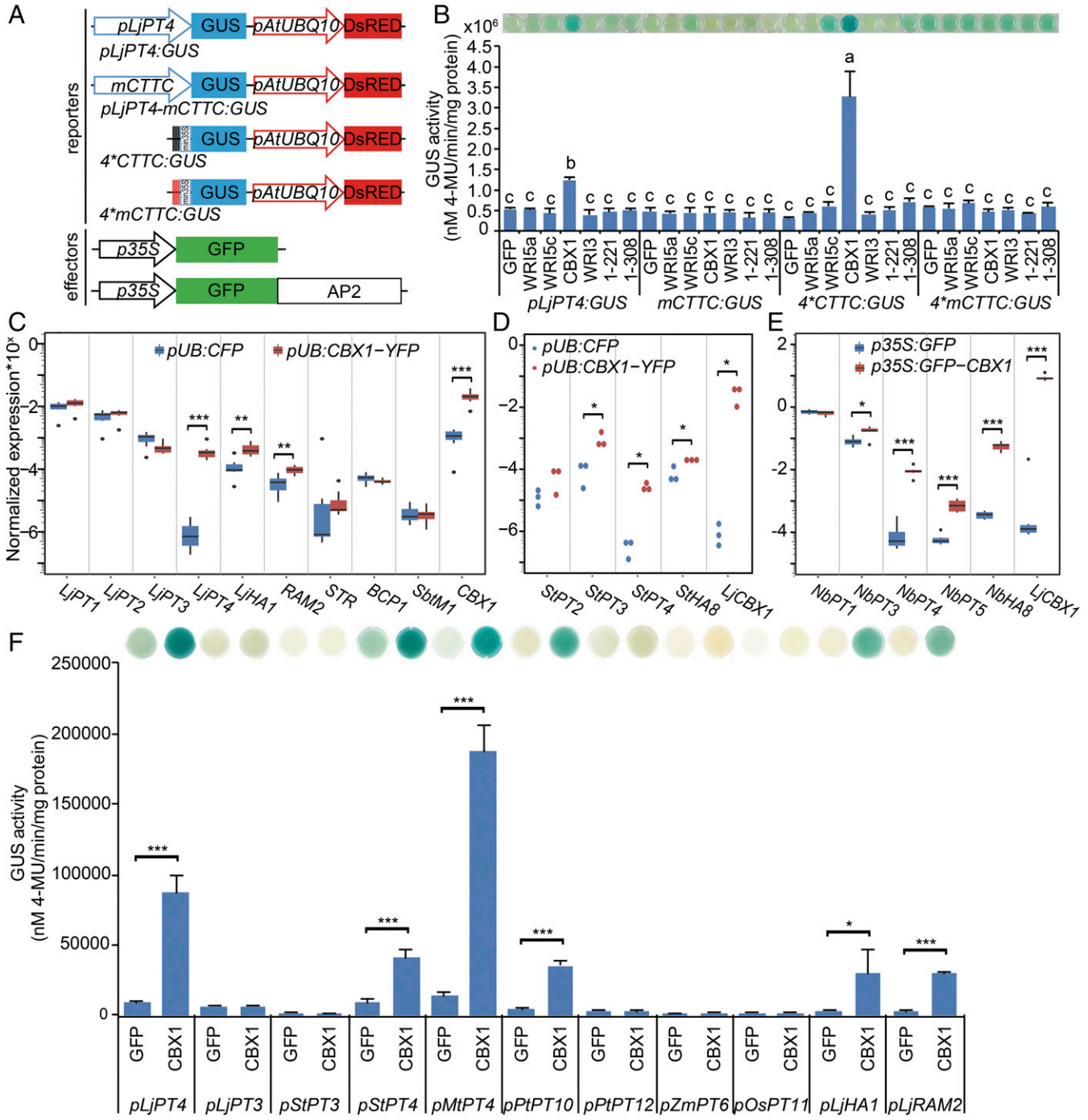

Fig. 3. CBX1 regulates mycorrhizal marker genes across different dicot species. (*A*) Diagram of reporter and effector utilized in the transactivation assay. DsRed was used to test transformation efficiency. *p35S:GFP*, negative control. (*B*) Transactivation assay with AP2 transcription factors on four chimeric reporter genes. GUS staining of suspension cultured cells is shown at the top of the graph. Mean ± SD ($n = 3$). One-way ANOVA followed by Tukey's HSD was performed ($F_{27.56} = 44.38$, $P < 0.001$). (*C*) Overexpression of CBX1 increased expression of *LjPT4*, *LjHA1*, and *RAM2* genes in *L. japonicus* in the absence of AM fungi. Box limits indicate the 25th and 75th percentiles. Bar-plot whiskers extend to the value that is no more than 1.5× interquartile range from the upper or lower quartile. Outliers were plotted by dots. Student's *t* test was used ($n = 7$). (*D*) Ectopic expression of CBX1 in hairy roots of potato led to transcript accumulation of mycorrhiza-induced Pi transporters and H^+-ATPase genes. Student's *t* test was used ($n = 3$). (*E*) Induction of MUP-related genes in ectopic expression of CBX1 in tobacco leaves. Student's *t* test was used ($n = 6$). $^*P < 0.05$; $^{**}P < 0.01$; $^{***}P < 0.001$. Three independent experiments were performed with similar results. (*F*) Transactivation by CBX1 of Pi transporter genes from different plant species, and of *L. japonicus LjHA1* and *RAM2* in *A. thaliana* suspension cultured cells. Mean values ± SD of GUS activity from three biological replicates are shown ($n = 3$; Student's *t* test; $^*P < 0.05$; $^{***}P < 0.001$). This experiment was repeated three times independently with similar results.

(*SI Appendix*, Fig. S5*C*), failed to activate the *LjPT4* and the *4*CTTC* synthetic promoter in *A. thaliana* cells (Fig. 3*B*). These results indicated that *LjPT4* promoter transactivation was dependent on the presence of the CBX1 carboxyl-terminal acidic region, the potential transactivation domain, encompassing amino acids 309–378 (40).

CBX1-CTTC CRE Regulation Mechanism Is Conserved in AM Host Species. Based on the proposed modular design of AM symbiosis (41), we hypothesized that CBX1 regulates a gene module to control mycorrhizal nutrient transport. To test this coregulation hypothesis, *CBX1* (*pUB:CBX1-YFP*) was ectopically expressed in transgenic *L. japonicus* hairy roots in the absence of AM fungi, which led to a significant increase in the level of *LjPT4* transcripts relative to the control, while *LjPT1*, *LjPT2*, and *LjPT3* remained unchanged (Fig. 3*C*). Membrane localized proton-ATPase (HA1) is essential for MPU through energizing proton-coupled Pht1 Pi transport (18, 19, 42). *LjHA1* expression was mycorrhiza inducible in roots (*SI Appendix*, Fig. S6*A*), and its promoter region containing the CTTC motif was directly bound by CBX1 (*SI Appendix*, Fig. S6*B*). Correspondingly, overexpression of *CBX1* in transformed roots led to a significant accumulation of *LjHA1* transcripts in the absence of AM fungi. Furthermore, ectopic expression of *L. japonicus CBX1* in transgenic hairy roots of *Solanum tuberosum* and in leaves of *Nicotiana benthamiana* led to a significant accumulation of mRNA encoding respective mycorrhiza-inducible Pi transporter and H^+-ATPase, respectively (Fig. 3 *D* and *E*). In sum, this suggested the conservation of *cis*-regulatory activity of CBX1 in mycorrhizal Pi uptake in diverse eudicot species.

Close homologs of CBX1 exist in different taxa (*SI Appendix*, Fig. S7). To test the hypothesis that the transcriptional regulatory mechanism controlled by CBX1 is evolutionarily conserved, promoters from mycorrhiza-inducible Pht1 genes *LjPT3*, *LjPT4*, *MtPT4*, potato *StPT3* and *StPT4*, poplar *PtPT10* and *PtPT12*, *OsPT11*, and *ZmPT6* were fused to the GUS reporter gene and were cotransformed with *CBX1* in *A. thaliana* suspension-cultured root cells (4, 9, 11, 12, 33, 43–45). Except *OsPT11*, all of the other eight genes comprise CTTC motifs in their promoters. In this in vivo system, CBX1 activated *LjPT4*, *StPT4*, *MtPT4*, and *PtPT10* promoters from Pht1 subfamily I genes, but not promoters from monocots, like *OsPT11* and *ZmPT6*, or from Pht1 subfamily III genes, including *StPT3*, *LjPT3*, and *PtPT12* (Fig. 3*F*). This activation of specific promoters from eudicot mycorrhizal hosts explains previous results obtained with the *OsPT11* promoter from rice, which was not activated when transformed into mycorrhizal potato and *M. truncatula* roots (5). CBX1 also induced GUS expression driven by the *LjHA1* gene promoter (Fig. 3*F*). Overall these data suggested the operation of a mycorrhizal gene module comprising CBX1, *LjPT4*, and *LjHA1* involved in MPU in eudicot plants.

Genome-Wide Targets of CBX1. In addition to *LjPT4* and *LjHA1*, transcript amounts of *RAM2* encoding glycerol-3-phosphate acyltransferase required for arbuscule development (46) were significantly increased (Fig. 3*C*), while expression of other mycorrhizal marker genes like *SbtM1*, *STR*, and *BCP1* was not affected (5, 47–49). CBX1 also activated the *RAM2* gene promoter (Fig. 3*F*), suggesting that CBX1 orchestrates expression of a wide array of genes involved in AM symbiosis development. We therefore investigated global DNA-binding sites of a CBX1-YFP fusion protein across the *L. japonicus* genome using chromatin immunoprecipitation coupled with high-throughput sequencing (ChIP-seq) (*SI Appendix*, Fig. S8 *A* and *B*). In total, 136 target genes belonged to the common intersect in two replicates, indicating high significance of the overlap between replicates (Fisher's exact test, odds ratio 184.95, $P < 2.2e\text{-}16$; Dataset S1). CBX1-binding sites were enriched near the transcription start site of target genes (Fig. 4*A*) and prevailed in promoters, 5′ UTR and intergenic regions (Fig. 4*B*). Functional annotation analysis showed that genes involved in lipid metabolism and transcription comprise a large proportion of the 136 CBX1 targets besides nonprotein coding and unknown genes (*SI Appendix*, Fig. S8*C*). Integrating our ChIP-seq analysis with comparative analysis of *L. japonicus* and *R. irregularis* gene regulation at transcript resolution (RNA-seq) (Dataset S2) (50) resulted in 43 CBX1 targets, which matched with mycorrhiza-inducible genes (Fisher's exact test, odds ratio 17.53, $P < 2.2e\text{-}16$) (Fig. 4*C* and Dataset S1), including *LjPT4* (Fig. 4*D*). ChIP-qPCR confirmed that the CBX1-YFP fusion protein had the ability to precipitate the region of *LjPT4* promoter containing CTTC CRE (Fig. 4 *E* and *F*). The CTTC-containing region in *LjPT3* was not enriched by CFP nor CBX1-YFP, which verified the ChIP-seq result. Consistent with *A. thaliana* WRI1 homolog (22, 23), 12 of 43 mycorrhiza-inducible CBX1 target genes refer to lipid metabolism and comprise nine genes involved in fatty acid biosynthesis [pyruvate dehydrogenase E1 subunit (*PDH_E1*α and *PDH_E1*β), dihydrolipoyl dehydrogenase 1 (*LPD1*), Biotin carboxyl carrier protein 2 (*BCCP2*), α-carboxyltransferase (α-*CT*), malonyl-CoA-ACP transacylase (*MAT*), acyl carrier protein1 (*ACP1*), enoyl-ACP reductase (*ENR*), and acyl ACP-thioesterase (*FatM*)] and three glycolytic genes [glycerol-3-phosphate dehydrogenase (*GPDH*), phosphoenolpyruvate/phosphate translocator (*PPT*), and pyruvate kinase isozyme G (*PK*)] (Fig. 4*G* and *SI Appendix*, Fig. S9). Recent research highlighted the important role of 16:0 fatty acid synthesis in mycorrhizal host plants and its presumed transfer to AM fungi to maintain the symbiosis (26–29, 51). Mycorrhizal induction of 11 lipid-related genes in *M. truncatula* is dependent on the activity of the GRAS regulator RAM1 (29). Eight of these genes were CBX1 targets in *L. japonicus*, including *BCCP2*, *PDH_E1*β, *PK*, *ACP1*, *MAT*, *ENR*, *GPDH*, and *PPT*. *RAM2* and *LjHA1* were not included in our 136 targets list due to incomplete genome sequence or presence only in one replicate experiment (*SI Appendix*, Fig. S13*C*). We therefore manually added the *RAM2* sequence to the *L. japonicus* genome sequence, and the ChIP-seq short sequence reads were sufficient for accurate mapping of enriched DNA fragments to *RAM2* (*SI Appendix*, Fig. S9). In sum, the results suggested that CBX1 has the ability to regulate genes underlying diverse AM functions including MPU and fatty acid biosynthesis.

AW box is enriched in CBX1-bound sites of lipid metabolic genes (Fig. 4*G* and *SI Appendix*, Fig. S9). CBX1 directly bound to the AW box in vitro (*SI Appendix*, Fig. S10*A*), which indicated conserved binding properties of WRI homologs. Overexpression of CBX1 significantly increased transcript levels of *BCCP2*, *PDHC_E1a*, *PDHC_E1*β, *LPD1*, *ENR*, *GPDH*, *ABCB*, *FatM*, and *Kelch* in *L. japonicus* (Fig. 4*H*). Likewise, the increased transcript amounts of fatty acid biosynthesis genes were also observed by ectopic expression of *CBX1* in tobacco leaves and in potato hairy roots (*SI Appendix*, Fig. S10 *B* and *C*), which stood in line with the specific accumulation of triacylglycerols in tobacco leaves after ectopic expression of *L. japonicus* CBX1, although total fatty acid contents were unchanged (*SI Appendix*, Fig. S11 *A* and *B*). In CBX1, both AP2 domains and the 212–308 region were required for binding to AW box and CTTC (Fig. 1 *E* and *F* and *SI Appendix*, Fig. S12*A*). Moreover, AW box acts in cooperation with CTTC in binding of the *LjPT4* promoter in vitro and its transactivation in vivo by CBX1 (Fig. 4*I* and *SI Appendix*, Fig. S12*B*). In sum, the results suggested CBX1-directed AM-specific gene regulation through direct binding to CTTC and AW box in the regulatory region of diverse target genes.

Besides MPU and lipid genes, transcripts of three GRAS genes encoding homologs to *M. truncatula* MIG1 (Lj6g3v1914570.1) (52) and MIG1-like proteins (Lj5g3v1598410.1 and Lj1g3v4851630.1) (34) were enriched by CBX1 (*SI Appendix*, Fig. S13 *A* and *B*), which placed CBX1 in a gene regulatory network of AM symbiosis. Overall, our findings showed that CBX1 coregulates different gene modules through its ability to recognize two motifs of divergent sequences, which mediates functions like the MPU and fatty acid biosynthesis and other still poorly explored interlinked processes involved in AM symbiosis.

Discussion

Reciprocal exchange of nutrients stabilizes the cooperation between mycobiont and phytobiont in the AM symbiosis over

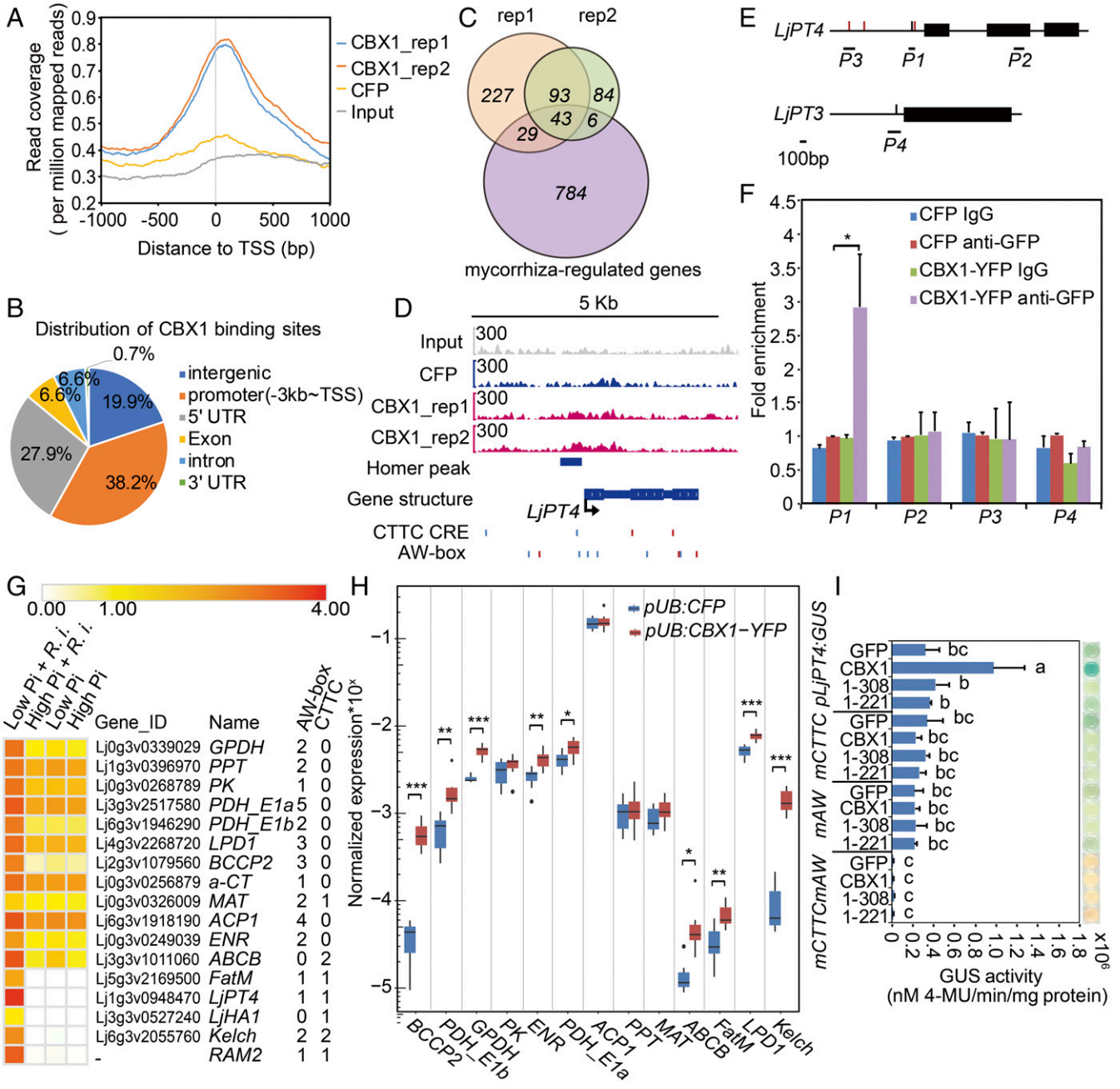

Fig. 4. Genome-wide identification of CBX1 target genes by ChIP-seq. (*A*) ChIP-seq analysis shows CBX1-binding peaks enriched near the transcription start site (TSS). The peaks shared in two replicate experiments were used. Immunoprecipitated DNA fragments from 1-mo-old hairy roots harboring *pUB:CBX1-YFP* or *pUB:CFP* negative control were subjected to DNA sequencing. (*B*) Distribution of 136 CBX1-binding sites in the *L. japonicus* genome. (*C*) Venn diagram depicting the overlap between CBX1 targets from ChIP-seq and mycorrhiza-regulated genes. Unique genes (392 and 226) were significantly enriched by CBX1 in two experiments (two times higher in surrounding 10-kb region; fold change relative to CFP control >2; $P < 0.0001$). rep, replicate. (*D*) IGV browser view of CBX1 binding on *LjPT4* gene. Tracks display data from Input, ChIPed CFP, and ChIPed CBX1 (two replicates) samples. Number on the upper left of each track indicates track height (300 reads per bin). Peak identified in Homer is indicated in blue bar. Thick lines represent exons and thin lines introns in gene structure. Black arrow indicates TSS. Blue and red ticks under the gene structure indicate CTTC core sequence (TCTTGT) or AW-box ($CnTnG(n)_7CG$) on the positive and negative DNA strand, respectively. (*E*) Schematic representation of genomic regions of *LjPT4* and *LjPT3* at scale. Black bars represent coding region. Lines represent noncoding DNA. CTTC CRE and AW box are indicated in promoter regions as black or red bars, respectively. P1 to P4 are DNA fragments designed for ChIP-qPCR. (*F*) Validation of ChIP-seq by ChIP-qPCR that CBX1 bound to the promoter of *LjPT4*. After normalization with input, fold enrichment was calculated, compared with anti-GFP ChIPed CFP. Mean values ± SD of three independent biological replicates were shown. Student's *t* test was used. $*P < 0.05$. (*G*) Mycorrhiza-inducible lipid-related genes were targeted by CBX1 in ChIP-seq. Heatmap of CBX1 target gene expression profiles based on $\log_{10}$ transformed counts per million (cpm) depicted from RNA-seq data analysis (50). The number of AW box and CTTC core (TCTTGT) were counted in the homer peaks from ChIP-seq. (*H*) Transcript accumulation of CBX1 targets in *L. japonicus* hairy root overexpressing CBX1 in the absence of AM fungi. Student's *t* test was used ($n = 7$). $*P < 0.05$; $**P < 0.01$; $***P < 0.001$. Three experiments were performed independently with similar results. (*I*) Transactivation assay with CBX1 on *pLjPT4:GUS* reporter with mutations on CTTC or/and AW box. Mean ± SD ($n = 3$). One-way ANOVA followed by Tukey's HSD was performed ($F_{15.32} = 14.17$, $P < 0.05$).

evolutionary time (53). With respect to the "biological market" theory (53, 54), regulators involved in orchestrating biological processes underlying mutualism, likely shared an important role in the evolution of AM symbiosis. We show here that mycorrhiza-inducible CBX1 from *L. japonicus*, a WRI1 transcription factor, acts as a regulator and activates genes encoding mycorrhiza-specific Pi transporter and proton-ATPase from diverse eudicot plants and proteins involved in fatty acid biosynthesis. The computational identification of the conserved CTTC CRE (TCTTGTT) (Fig. 1*C*) (14) through cross-species comparison of mycorrhizal-regulated genes was consistent with the binding specificity of CBX1 to TCTTGT core sequence shown through EMSA (Fig. 1*D*). Transactivation assays in suspension cultured cells of nonmycorrhizal host *A. thaliana* and CBX1 overexpression studies in transformed roots or leaves from *L. japonicus*, potato, and tobacco in the absence of AM fungi suggests the presence of a conserved regulatory mechanism controlling simultaneous expression of Pht1 subfamily I genes and proton-ATPase genes in eudicots. Failure of CBX1 to bind in vivo (Fig. 4*F*) nor activate (Fig. 3*F*) the promoter of *LjPT3*, which also contains a CTTC motif, suggested an important role of sequences flanking the CTTC motif in *cis* regulation. Significantly reduced but not abolished GUS activity driven by *LjPT4*-mCTTC in transgenic roots also suggested the existence of alternative CREs (Fig. 1*A*). Cooccurrence of the CTTC motif and AW box was found in the promoters of several mycorrhiza-specific and mycorrhiza–up-regulated genes (Fig. 4*G*). CBX1 could bind to both motifs (Fig. 1 and *SI Appendix*, Figs. S9, S10*A*, and S12), and CBX1-mediated activation of *LjPT4* was dependent on both motifs (Fig. 4*I*), implying that the two motifs build a molecular module in AM symbiosis genes. The precise regulatory function of CBX1 on the CTTC/AW molecular module of individual target gene awaits further exploration. Remaining mycorrhizal gene expression in *cbx1* mutants (Fig. 2*B*) suggested that other transcription factors could function redundantly, such as AM-inducible *WRI5a/b/c* (29, 34) with CTTC-binding ability (*SI Appendix*, Fig. S2).

Genome-wide identification of CBX1-binding sites through ChIP-seq revealed 43 mycorrhiza-inducible targets of CBX1 (Dataset S1). Among those, 12 genes are involved in de novo fatty acid synthesis and glycolysis. Enrichment of the AW box in these binding regions supported the conserved regulation of lipid synthesis by WRI-like proteins across diverse plant species (23, 55). In the 43-gene list, genes encoding LjPT4, FatM (an AMP-dependent synthetase and ligase), and an ABC transporter B family (*ABCB*) protein were conserved in phylogenetically diverse mycorrhizal host species (56). In addition, we showed that *LjHA1* was directly regulated by CBX1, as CBX1 had the ability to bind the TCTTGT-containing promoter region of *LjHA1* in vitro (*SI Appendix*, Fig. S6*B*) and activated the *pLjHA1:GUS* chimeric gene in *A. thaliana* cells (Fig. 3*F*). The two CBX1 targets *RAM2* and *LjHA1* were initially not identified in our ChIP-seq analysis, which suggested that some targets were missed, owing to incomplete genome information or annotation errors, technical impediments, or harsh criteria for selecting peaks through the Homer pipeline (*SI Appendix*, Figs. S9 and S13*C*). Besides, *MIG1*, a regulator of root cortical cell expansion required for arbuscule development (52), was identified as a CBX1 target gene through ChIP-seq and ChIP-qPCR (*SI Appendix*, Fig. S13 *A* and *B*). In *M. truncatula*, the 230-bp truncated promoter of *MIG1* containing two CTTC motifs but lacking AW box was sufficient to drive GUS expression in response to AM fungi (52). As overexpression of CBX1 was used for ChIP-seq in the absence of AM fungi, further research will verify the function of specific CBX1 targets in mycorrhizal symbiosis.

LjPT4, *LjHA1*, and *RAM2* genes were shown to be regulated by GRAS protein RAM1 (29, 57, 58), which is directly regulated by the CCaMK–CYCLOPS–DELLA complex (49). More research is required to elucidate whether CBX1 participates in mycorrhizal gene expression independently, cooperatively, or downstream of RAM1 during AM development. Continued investigations into how CBX1 and orthologous proteins evolved from early land plants and their algal ancestor (41) will help to understand the evolution of regulatory modules that determine mutualistic interactions at the root-fungus interface in AM symbiosis.

Materials and Methods

Details of plant materials and growth conditions are provided in *SI Appendix*. Transformation of hairy roots and leaves, protein purification and EMSA, quantitative real-time PCR analysis, phylogenetic analysis, histochemical GUS analysis, transactivation assay, subcellular protein localization, ChIP-seq, and RNA-seq data analysis are described in *SI Appendix, SI Materials and Methods*. Constructs and primers are listed in *SI Appendix*, Tables S1–S6. CBX1 targets and their functional annotation are listed in Dataset S1. Genes responsive to *R. irregularis* in *L. japonicus* were identified using RNA-seq as described before (50) and are listed in Dataset S2.

ACKNOWLEDGMENTS. We thank Dr. K. Schlücking and V. Wewer, Y. Arlt, and C. Nothelle for experimental support; Dr. I. Fabianska for assistance with statistical data analysis; Dr. M. Böhmer (Muenster University) for support with EMSA; Dr. N. Gerlach for providing plasmid *pRedRoot-pZmPT6:GUS*; Dr. F. Martin (Institut National de la Recherche Agronomique) for providing poplar genomic DNA; Drs. F. He, and U. Höcker for helpful discussions; and S. Werth for photographs. This research was supported by an Alexander von Humboldt foundation research fellowship (to L.X.), a grant from The Institute for the Promotion of Teaching Science and Technology Thailand (to L.K.), International Max Planck Research School on "Understanding Complex Plant Traits using Computational and Evolutionary Approaches" in Cologne (to G.S.), and German Science Foundation Grant BU-2250/12-1 (to M. Bucher)

1. Remy W, Taylor TN, Hass H, Kerp H (1994) Four hundred-million-year-old vesicular arbuscular mycorrhizae. *Proc Natl Acad Sci USA* 91:11841–11843.
2. Gutjahr C, Parniske M (2013) Cell and developmental biology of arbuscular mycorrhiza symbiosis. *Annu Rev Cell Dev Biol* 29:593–617.
3. Smith SE, Smith FA, Jakobsen I (2003) Mycorrhizal fungi can dominate phosphate supply to plants irrespective of growth responses. *Plant Physiol* 133:16–20.
4. Harrison MJ, Dewbre GR, Liu J (2002) A phosphate transporter from Medicago truncatula involved in the acquisition of phosphate released by arbuscular mycorrhizal fungi. *Plant Cell* 14:2413–2429.
5. Pumplin N, Harrison MJ (2009) Live-cell imaging reveals periarbuscular membrane domains and organelle location in Medicago truncatula roots during arbuscular mycorrhizal symbiosis. *Plant Physiol* 151:809–819.
6. Kobae Y, Hata S (2010) Dynamics of periarbuscular membranes visualized with a fluorescent phosphate transporter in arbuscular mycorrhizal roots of rice. *Plant Cell Physiol* 51:341–353.
7. Javot H, Penmetsa RV, Terzaghi N, Cook DR, Harrison MJ (2007) A Medicago truncatula phosphate transporter indispensable for the arbuscular mycorrhizal symbiosis. *Proc Natl Acad Sci USA* 104:1720–1725.
8. Yang SY, et al. (2012) Nonredundant regulation of rice arbuscular mycorrhizal symbiosis by two members of the phosphate transporter1 gene family. *Plant Cell* 24:4236–4251.
9. Willmann M, et al. (2013) Mycorrhizal phosphate uptake pathway in maize: Vital for growth and cob development on nutrient poor agricultural and greenhouse soils. *Front Plant Sci* 4:533.
10. Walder F, et al. (2015) Plant phosphorus acquisition in a common mycorrhizal network: regulation of phosphate transporter genes of the Pht1 family in sorghum and flax. *New Phytol* 205:1632–1645.
11. Loth-Pereda V, et al. (2011) Structure and expression profile of the phosphate Pht1 transporter gene family in mycorrhizal Populus trichocarpa. *Plant Physiol* 156:2141–2154.
12. Nagy R, et al. (2005) The characterization of novel mycorrhiza-specific phosphate transporters from Lycopersicon esculentum and Solanum tuberosum uncovers functional redundancy in symbiotic phosphate transport in solanaceous species. *Plant J* 42:236–250.
13. Chen A, et al. (2011) Identification of two conserved cis-acting elements, MYCS and P1BS, involved in the regulation of mycorrhiza-activated phosphate transporters in eudicot species. *New Phytol* 189:1157–1169.
14. Lota F, et al. (2013) The cis-acting CTTC-P1BS module is indicative for gene function of LjVTI12, a Qb-SNARE protein gene that is required for arbuscule formation in Lotus japonicus. *Plant J* 74:280–293.
15. Karandashov V, Nagy R, Wegmuller S, Amrhein N, Bucher M (2004) Evolutionary conservation of a phosphate transporter in the arbuscular mycorrhizal symbiosis. *Proc Natl Acad Sci USA* 101:6285–6290.
16. Xie X, et al. (2013) Functional analysis of the novel mycorrhiza-specific phosphate transporter AsPT1 and PHT1 family from Astragalus sinicus during the arbuscular mycorrhizal symbiosis. *New Phytol* 198:836–852.
17. Bucher M (2007) Functional biology of plant phosphate uptake at root and mycorrhiza interfaces. *New Phytol* 173:11–26.

18. Krajinski F, et al. (2014) The H+-ATPase HA1 of Medicago truncatula is essential for phosphate transport and plant growth during arbuscular mycorrhizal symbiosis. *Plant Cell* 26:1808–1817.
19. Wang E, et al. (2014) A H+-ATPase that energizes nutrient uptake during mycorrhizal symbioses in rice and Medicago truncatula. *Plant Cell* 26:1818–1830.
20. Liu J, et al. (2016) Analysis of tomato plasma membrane H(+)-ATPase gene family suggests a mycorrhiza-mediated regulatory mechanism conserved in diverse plant species. *Mycorrhiza* 26:645–656.
21. Licausi F, Ohme-Takagi M, Perata P (2013) APETALA2/ethylene responsive factor (AP2/ERF) transcription factors: Mediators of stress responses and developmental programs. *New Phytol* 199:639–649.
22. To A, et al. (2012) WRINKLED transcription factors orchestrate tissue-specific regulation of fatty acid biosynthesis in Arabidopsis. *Plant Cell* 24:5007–5023.
23. Maeo K, et al. (2009) An AP2-type transcription factor, WRINKLED1, of Arabidopsis thaliana binds to the AW-box sequence conserved among proximal upstream regions of genes involved in fatty acid synthesis. *Plant J* 60:476–487.
24. Cernac A, Benning C (2004) WRINKLED1 encodes an AP2/EREB domain protein involved in the control of storage compound biosynthesis in Arabidopsis. *Plant J* 40: 575–585.
25. Baud S, et al. (2007) WRINKLED1 specifies the regulatory action of LEAFY COTYLEDON2 towards fatty acid metabolism during seed maturation in Arabidopsis. *Plant J* 50: 825–838.
26. Jiang Y, et al. (2017) Plants transfer lipids to sustain colonization by mutualistic mycorrhizal and parasitic fungi. *Science* 356:1172–1175.
27. Keymer A, et al. (2017) Lipid transfer from plants to arbuscular mycorrhiza fungi. *eLife* 6:29107.
28. Bravo A, Brands M, Wewer V, Dörmann P, Harrison MJ (2017) Arbuscular mycorrhiza-specific enzymes FatM and RAM2 fine-tune lipid biosynthesis to promote development of arbuscular mycorrhiza. *New Phytol* 214:1631–1645.
29. Luginbuehl LH, et al. (2017) Fatty acids in arbuscular mycorrhizal fungi are synthesized by the host plant. *Science* 356:1175–1178.
30. Pfeffer PE, Douds DD, Jr, Becard G, Shachar-Hill Y (1999) Carbon uptake and the metabolism and transport of lipids in an arbuscular mycorrhiza. *Plant Physiol* 120: 587–598.
31. Bago B, Pfeffer PE, Shachar-Hill Y (2000) Carbon metabolism and transport in arbuscular mycorrhizas. *Plant Physiol* 124:949–958.
32. Devers EA, Teply J, Reinert A, Gaude N, Krajinski F (2013) An endogenous artificial microRNA system for unraveling the function of root endosymbioses related genes in Medicago truncatula. *BMC Plant Biol* 13:82.
33. Volpe V, Giovannetti M, Sun XG, Fiorilli V, Bonfante P (2016) The phosphate transporters LjPT4 and MtPT4 mediate early root responses to phosphate status in non mycorrhizal roots. *Plant Cell Environ* 39:660–671.
34. Xue L, et al. (2015) Network of GRAS transcription factors involved in the control of arbuscule development in Lotus japonicus. *Plant Physiol* 167:854–871.
35. Guether M, et al. (2009) Genome-wide reprogramming of regulatory networks, transport, cell wall and membrane biogenesis during arbuscular mycorrhizal symbiosis in Lotus japonicus. *New Phytol* 182:200–212.
36. Handa Y, et al. (2015) RNA-seq transcriptional profiling of an arbuscular mycorrhiza provides insights into regulated and coordinated gene expression in Lotus japonicus and Rhizophagus irregularis. *Plant Cell Physiol* 56:1490–1511.
37. Sugimura Y, Saito K (2017) Transcriptional profiling of arbuscular mycorrhizal roots exposed to high levels of phosphate reveals the repression of cell cycle-related genes and secreted protein genes in Rhizophagus irregularis. *Mycorrhiza* 27:139–146.
38. Breuillin F, et al. (2010) Phosphate systemically inhibits development of arbuscular mycorrhiza in Petunia hybrida and represses genes involved in mycorrhizal functioning. *Plant J* 64:1002–1017.
39. Nagy R, Drissner D, Amrhein N, Jakobsen I, Bucher M (2009) Mycorrhizal phosphate uptake pathway in tomato is phosphorus-repressible and transcriptionally regulated. *New Phytol* 181:950–959.
40. Ma W, et al. (2015) Deletion of a C-terminal intrinsically disordered region of WRINKLED1 affects its stability and enhances oil accumulation in Arabidopsis. *Plant J* 83:864–874.
41. Delaux PM, et al. (2015) Algal ancestor of land plants was preadapted for symbiosis. *Proc Natl Acad Sci USA* 112:13390–13395.
42. Karandashov V, Bucher M (2005) Symbiotic phosphate transport in arbuscular mycorrhizas. *Trends Plant Sci* 10:22–29.
43. Paszkowski U, Kroken S, Roux C, Briggs SP (2002) Rice phosphate transporters include an evolutionarily divergent gene specifically activated in arbuscular mycorrhizal symbiosis. *Proc Natl Acad Sci USA* 99:13324–13329.
44. Maeda D, et al. (2006) Knockdown of an arbuscular mycorrhiza-inducible phosphate transporter gene of Lotus japonicus suppresses mutualistic symbiosis. *Plant Cell Physiol* 47:807–817.
45. Rausch C, et al. (2001) A phosphate transporter expressed in arbuscule-containing cells in potato. *Nature* 414:462–470.
46. Wang E, et al. (2012) A common signaling process that promotes mycorrhizal and oomycete colonization of plants. *Curr Biol* 22:2242–2246.
47. Zhang Q, Blaylock LA, Harrison MJ (2010) Two Medicago truncatula half-ABC transporters are essential for arbuscule development in arbuscular mycorrhizal symbiosis. *Plant Cell* 22:1483–1497.
48. Takeda N, Haage K, Sato S, Tabata S, Parniske M (2011) Activation of a Lotus japonicus subtilase gene during arbuscular mycorrhiza is dependent on the common symbiosis genes and two cis-active promoter regions. *Mol Plant Microbe Interact* 24: 662–670.
49. Pimprikar P, et al. (2016) A CCaMK-CYCLOPS-DELLA complex activates transcription of RAM1 to regulate arbuscule branching. *Curr Biol* 26:1126.
50. Vijayakumar V, et al. (2016) Integrated multi-omics analysis supports role of lysophosphatidylcholine and related glycerophospholipids in the Lotus japonicus-Glomus intraradices mycorrhizal symbiosis. *Plant Cell Environ* 39:393–415.
51. Brands M, Wewer V, Keymer A, Gutjahr C, Dörmann P (2018) The Lotus japonicus acyl-acyl Carrier protein thioesterase FatM is required for mycorrhiza formation and lipid accumulation of Rhizophagus irregularis. *Plant J* 95:219–232.
52. Heck C, et al. (2016) Symbiotic fungi control plant root cortex development through the novel GRAS transcription factor MIG1. *Curr Biol* 26:2770–2778.
53. Kiers ET, et al. (2011) Reciprocal rewards stabilize cooperation in the mycorrhizal symbiosis. *Science* 333:880–882.
54. Kiers ET, et al. (2016) Misconceptions on the application of biological market theory to the mycorrhizal symbiosis. *Nat Plants* 2:16063.
55. Pouvreau B, et al. (2011) Duplicate maize Wrinkled1 transcription factors activate target genes involved in seed oil biosynthesis. *Plant Physiol* 156:674–686.
56. Bravo A, York T, Pumplin N, Mueller LA, Harrison MJ (2016) Genes conserved for arbuscular mycorrhizal symbiosis identified through phylogenomics. *Nat Plants* 2: 15208.
57. Park HJ, Floss DS, Levesque-Tremblay V, Bravo A, Harrison MJ (2015) Hyphal branching during arbuscule development requires reduced arbuscular mycorrhiza1. *Plant Physiol* 169:2774–2788.
58. Gobbato E, et al. (2012) A GRAS-type transcription factor with a specific function in mycorrhizal signaling. *Curr Biol* 22:2236–2241.